Summertime land-atmosphere interactions in response to anomalous springtime snow cover in northern Eurasia

Shinji Matsumura,[1] Koji Yamazaki,[1] and Tatsushi Tokioka[2]

Received 27 April 2009; revised 24 June 2010; accepted 29 June 2010; published 21 October 2010.

[1] An atmospheric general circulation model (AGCM) is used to investigate the effects of springtime high-latitude snow cover on the summertime climate system in the form of land-atmosphere interactions in northern Eurasia. We performed light and heavy snow runs in which the initial snow mass in northern Eurasia was varied. Significant differences in model response between the light and heavy snow runs are evident in terms of not only land surface parameters but also summertime northern atmospheric circulation. Changes in the initial snow cover have a strong effect on the simulated surface air temperature. In western Siberia, the albedo of the snow cover makes a strong contribution to the difference in surface heating between the runs, because snow mass anomalies are still present over western Siberia in June. In eastern Siberia (the Lena Basin), where the snow disappears in June in both runs, the snow-hydrological effect is prominent throughout summer. The increased soil moisture in the heavy snow run causes increased evaporation, resulting in turn in surface cooling. The initial soil moisture content is dry in eastern Siberia and wet in western Siberia, resulting in contrasting responses between the two regions. In the light snow run, the subpolar jet is strengthened and maintained along the Arctic coast in early summer, and wave activity propagates eastward over northern Eurasia. Changes in the atmospheric circulation generate an east-west dipole structure of precipitation anomalies over northern Eurasia. These results suggest that variations in the springtime Eurasian snow mass result in changes in the summertime northern atmospheric circulation and hydrological cycle via land-atmosphere interactions.

Citation: Matsumura, S., K. Yamazaki, and T. Tokioka (2010), Summertime land-atmosphere interactions in response to anomalous springtime snow cover in northern Eurasia, *J. Geophys. Res.*, *115*, D20107, doi:10.1029/2009JD012342.

1. Introduction

[2] The Siberian Subarctic has the latest snowmelt in northern Eurasia. Figure 1 shows the mean number of days with snow cover as observed using the special sensor microwave/imager (SSM/I). Snow covers large regions of northern Siberia in May, but it largely disappears in June, except in the Arctic coastal region, especially western Siberia. In terms of analyzing variations in snow cover caused by atmospheric circulation, several observational studies have established a fundamental relationship between atmospheric conditions and the timing of snow disappearance [e.g., *Shinoda et al.*, 2001; *Iijima et al.*, 2007] and a relationship between the wintertime North Atlantic Oscillation (NAO) or Arctic Oscillation (AO) and subsequent springtime snow cover [e.g., *Bojariu and Gimeno*, 2003; *Ogi et al.*, 2003; *Schaefer et al.*, 2004].

[3] As snowmelt progresses, the surface air temperature in northern Siberia rapidly increases, reaching a maximum in July (Figure 2). The surface air temperature gradient across the Arctic coast also reaches a maximum in July as the surface air temperature of the Arctic Ocean remains low owing to the presence of sea ice. In August, the surface air temperature begins to decrease and the land-sea contrast weakens slightly. As a result, the subpolar jet, which is accompanied by enhanced eddy activity, is observed in early summer, forming a double-jet structure together with the subtropical jet [e.g., *Serreze et al.*, 2001]. The subpolar jet acts as a stationary Rossby waveguide, and *Nakamura and Fukamachi* [2004] reported that a wave packet emanates from Europe to the Far East along the Arctic coast. They also suggested that a stationary Rossby wave contributes to the formation of an upper-level ridge over eastern Siberia, leading to the development of the surface Okhotsk high [*Wang and Yasunari*, 1994; *Tachibana et al.*, 2004], which commonly brings an abnormally cool summer to East Asia. *Arai and Kimoto* [2005] reported the effects of the springtime surface temperature in Siberia on the enhancement of

[1] Faculty of Environmental Earth Science, Hokkaido University, Sapporo, Japan.
[2] Japan Agency for Marine-Earth Science and Technology, Yokohama, Japan.

0148-0227/10/2009JD012342

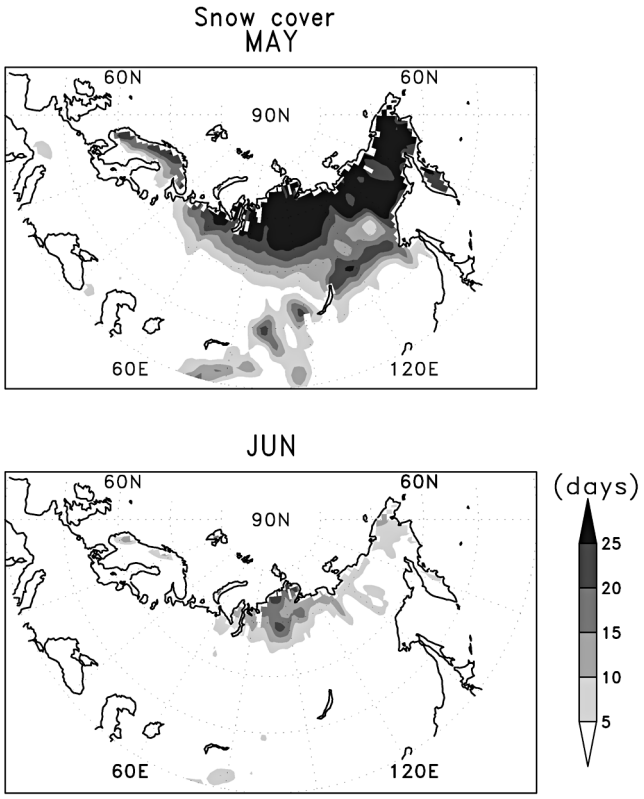

Figure 1. The mean number of days with snow cover in May and June observed by SSM/I for the period 1987–2004. Data were obtained from Japan Meteorological Agency analyses.

blocking activity in early summer, which is associated with intensification of the surface Okhotsk high.

[4] The relationship between Eurasian snow cover and summertime atmospheric circulation has been investigated by many researchers. In particular, sensitivity experiments have been performed using atmospheric general circulation models (AGCMs) to examine the responses of midlatitude summer monsoons to anomalous Eurasian snow cover in early spring [e.g., *Barnett et al.*, 1989; *Yasunari et al.*, 1991; *Vernekar et al.*, 1995; *Douville and Royer*, 1996]. Snow produces two types of effects on the climate: the albedo effect and the soil moisture effect. The albedo effect is related to the extent of snow cover, and the soil moisture effect is related to snow depth. *Shen et al.* [1998] confirmed that northern snow signals north of 50°N do not significantly affect the following Asian summer monsoon. In an observational study of the influence of northern snow cover, *Kodera and Chiba* [1989] found that springtime Eurasian snow cover anomalies are related to the intensity of the stationary summer Okhotsk ridge, which exerts a significant influence on the summer climate of Eurasia.

[5] Many previous studies on the snow-monsoon relationship have focused on midlatitude snow cover, yet few studies have investigated the influence of high-latitude snow cover on the summertime climate system via land-atmosphere interactions without separating the atmosphere and land processes in northern Eurasia. It is unclear to what extent the snow cover is coupled with the atmosphere and what processes are responsible for changes in local as well as large-scale climate systems due to regional snow cover anomalies in the northern snow signals.

[6] The purpose of the present study is to examine the effect of anomalous springtime snow cover in northern Eurasia on the summertime high-latitude climate system in Eurasia. To this end, we performed a sensitivity experiment using a high-resolution AGCM to analyze in detail the regional land-atmosphere climate system. The remainder of this paper is organized as follows. Section 2 describes the model and experiments. Section 3 describes changes in the surface conditions and compares the surface heat and water budgets between western and eastern Siberia. Section 4 discusses changes in atmospheric circulation and the hydrological cycle, and section 5 presents a discussion of the results. Finally, the main conclusions are given in section 6.

2. Model and Experiments

2.1. Model

[7] The AGCM used in this study was jointly developed by the Center for Climate System Research (CCSR) of the University of Tokyo, Japan, and the National Institute for Environmental Studies (NIES), Japan. It is a global spectral model with a triangular truncation in the horizontal direction and a sigma coordinate in the vertical direction. The cumulus parameterization scheme developed by *Arakawa and Schubert* [1974] is used with simplifications. Cumulus convection and large-scale condensation account for precipitation; the distinction between rain and snow is made on

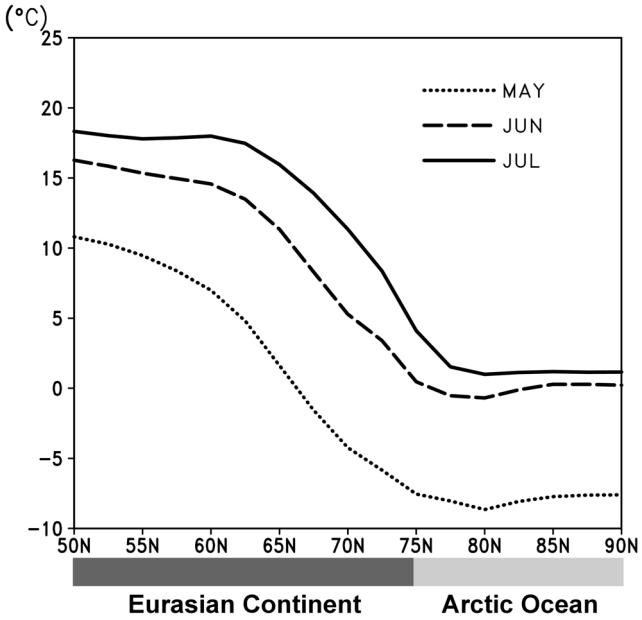

Figure 2. Latitudinal distribution of mean surface air (2 m) temperature (°C) for the period 1979–2002 across the Siberian Arctic coast from May to July, zonally averaged from 60°E to 120°E. Data are obtained from ECMWF reanalysis (ERA-40).

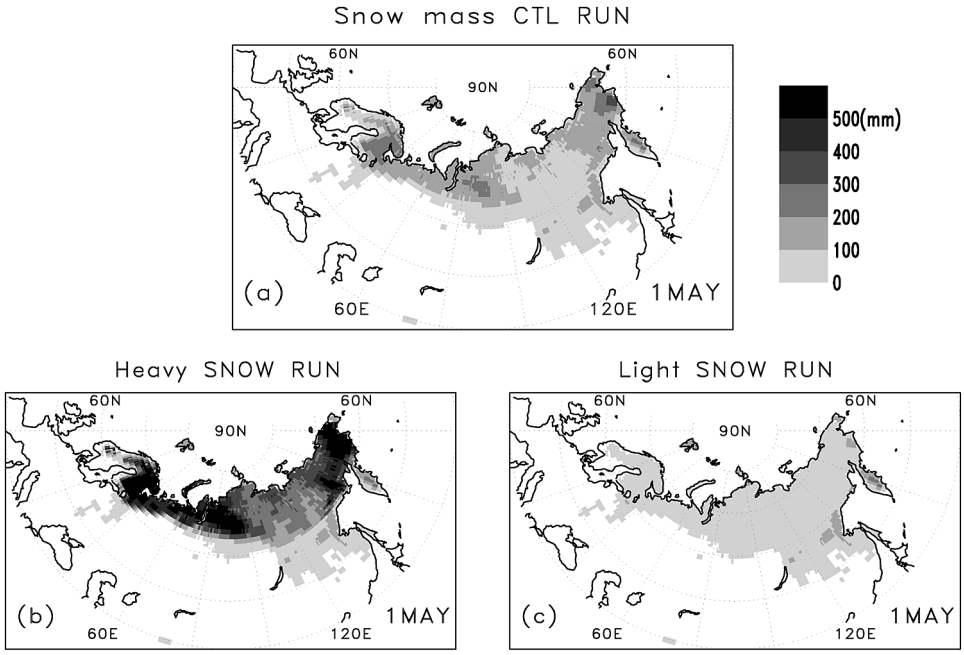

Figure 3. Distribution of snow mass (mm) on May 1 under initial atmospheric conditions. (a) Control run. (b) Heavy snow run, i.e., the snow mass is thrice that in Figure 3a. (c) Light snow run, i.e., the snow mass is one third of that in Figure 3a.

the basis of the surface air temperature. In addition to the usual atmospheric variables, the model predicts soil moisture, soil temperature, and snow amount. Parameterization of land surface processes is carried out by adopting a three-layer model for temperature and a one-layer model for soil moisture. The surface skin temperature is implicitly estimated from the surface energy balance of an infinitesimally thin layer, and the ground temperature is prognostically calculated by a diffusion scheme. Evaporation from the surface is calculated using a bulk formula, and evaporation efficiency is estimated from soil moisture W_g, which in turn is predicted using a simple bucket model with a field capacity of 200 kg m^{-2} (corresponding to a bucket with 200 mm depth):

$$\rho_w \frac{\partial W_g}{\partial t} = P_{rain} + M_s - (1 - f_s)E - R, \tag{1}$$

where P_{rain} is the precipitation in liquid form; M_s is snowmelt; E is evaporation; f_s is the snow cover fraction, which is represented as a function of snow mass; R is runoff flux; and ρ_w is the density of water. Runoff occurs whenever the soil moisture exceeds the saturation soil moisture W^* (200 kg m^{-2}) to maintain $W_g \leq W^*$. The snow mass W_s (water equivalent) is prognostically determined by the balance between snowfall P_{snow} and snowmelt M_s:

$$\rho_s \frac{\partial W_s}{\partial t} = P_{snow} - f_s E - M_s. \tag{2}$$

The snow layer is considered a part of the uppermost layer of the soil. Thus, the heat content of the first layer and the heat conductivity between the first layer and underlying layers are modified by the presence of snow. Surface albedo α of the snow-covered ground is represented as a function of the snow mass W_s:

$$\alpha = \begin{cases} \alpha' + (\alpha_s - \alpha')\sqrt{W_s/W_c} & W_s < W_c, \\ \alpha_s & W_s \geq W_c, \end{cases} \tag{3}$$

where W_c is the critical snow amount, fixed at 100 kg m^{-2}; α_s denotes the snow albedo, which varies from 0.5 (melting snow) to 0.7 (deep snow); and α' represents the bare land albedo, which depends on land type. Details of the model and an evaluation of its performance can be found in *Numaguti* [1999].

2.2. Experimental Design

[8] The model has a horizontal resolution of T106 (triangular truncation at wave number 106); the corresponding grid interval is approximately 1°, and the number of grid levels is 20 in the vertical direction. An ensemble experiment is performed with 10 independent integrations from April 21–30 to the end of August with the prescribed climatological sea surface temperature (SST). The initial atmospheric conditions for 21–30 April 1993 were obtained from the National Centers for Environmental Prediction (NCEP) and National Center for Atmospheric Research (NCAR) reanalyses [*Kalnay et al.*, 1996]. The initial soil moisture content is computed in a control run on May 1 in a given year. The snow cover in the control run (Figure 3a) reasonably reproduces the climatology (Figure 1) observed by SSM/I over northern Eurasia in May (i.e., high snow in western and far-eastern Siberia and low snow in eastern Siberia), although snow disappearance is slightlyearly.

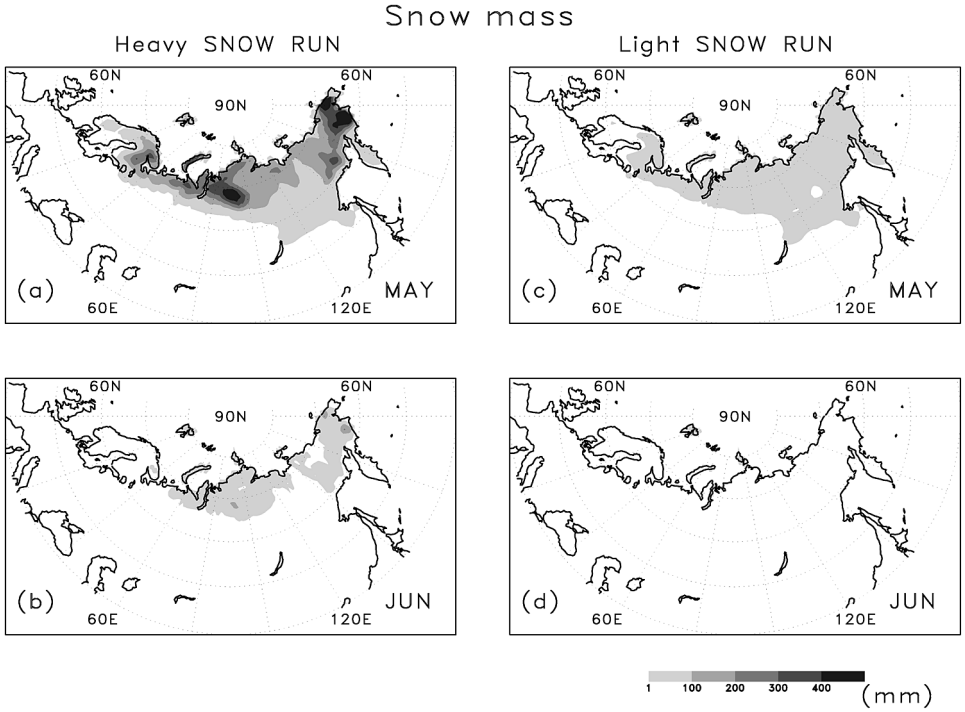

Figure 4. Distribution of snow mass (mm) in the heavy snow run in (a) May and (b) June. The distribution of snow mass (mm) in the light snow run in (c) May and (d) June.

Similarly, the atmospheric circulation in the control run adequately reproduces the observed climatology (not shown).

[9] We performed a 10-member heavy snow run (i.e., a late snowmelt run) and a 10-member light snow run (an early snowmelt run). The relatively large initial snow anomalies between light and heavy snow runs are given, as it is then easy to detect the model responses to snowmelt. For the heavy snow run (Figure 3b), we prescribed an initial snow mass (water equivalent) that is thrice that in the control run (Figure 3a) on May 1 (same year as the initial soil moisture) and north of 60°N in the snow-covered region of the Eurasian continent. Similarly, an initial snow mass that is one third that in the control run is prescribed for the light snow run (Figure 3c). The initial snow mass is given for all 10 ensemble members on May 1.

[10] In eastern Siberia, snowmelt begins 30 days before the day of snow disappearance and accelerates during the last 10 days prior to disappearance [*Iijima et al.*, 2007]. Thus, snow depth shows marked changes during the melting period in early and late snowmelt years. Indeed, the variation in snow depth in northern Eurasia is larger than the variations in central Eurasia, and the ratio of snow depth in late snowmelt years to that in early snowmelt years is approximately 9 in late April [*Shinoda et al.*, 2001, Figure 8]. Therefore, the initial snow anomalies are similar to the usual range of natural variations.

[11] The differences between the light snow run and control run (light snow – control runs) and the differences between the heavy snow run and control run (heavy snow – control runs) show opposite signs in our experiment (not shown). This indicates that the model shows a linear response to the anomalous snow mass. Because the control run is only one realization, herein we discuss the anomalies between the light and heavy snow runs to emphasize the model responses to the initial snow mass, andthe anomalies are defined as the differences (light – heavy snow run) in the ensemble means of 10 members in both the light and heavy snow runs.

3. Thermal and Hydrological Changes at the Surface

3.1. Changes in Surface Conditions

[12] Figure 4 shows the distribution of snow mass in the heavy and light snow runs for May and June. In the light snow run, the snow mass over the Eurasian continent disappears in June (Figure 4d), whereas in the heavy snow run, the snow mass remains until June (Figure 4b). The change in the initial snow condition has a strong effect on the simulated surface air temperature. Figure 5 shows the surface air temperature (T_S) anomalies (light – heavy snow runs) from May to August. Positive T_S anomalies are clearly seen only over northern Eurasia in May, whereas in June they are restricted to western Siberia (the Ob and Yenisey basins) and northeastern Siberia. Although the T_S anomalies over most of Eurasia disappear in July, another large T_S anomaly emerges at around 120°E over eastern Siberia (the Lena Basin) in July and August.

[13] Snow cover has a marked effect on the land surface temperature and atmospheric circulation as a consequence of various physical processes [*Groisman et al.*, 1994]. The high albedo of snow cover results in reduced net incoming solar radiation,which in turn results in a decrease in surface heating of the continent. The high land-surface albedo in the

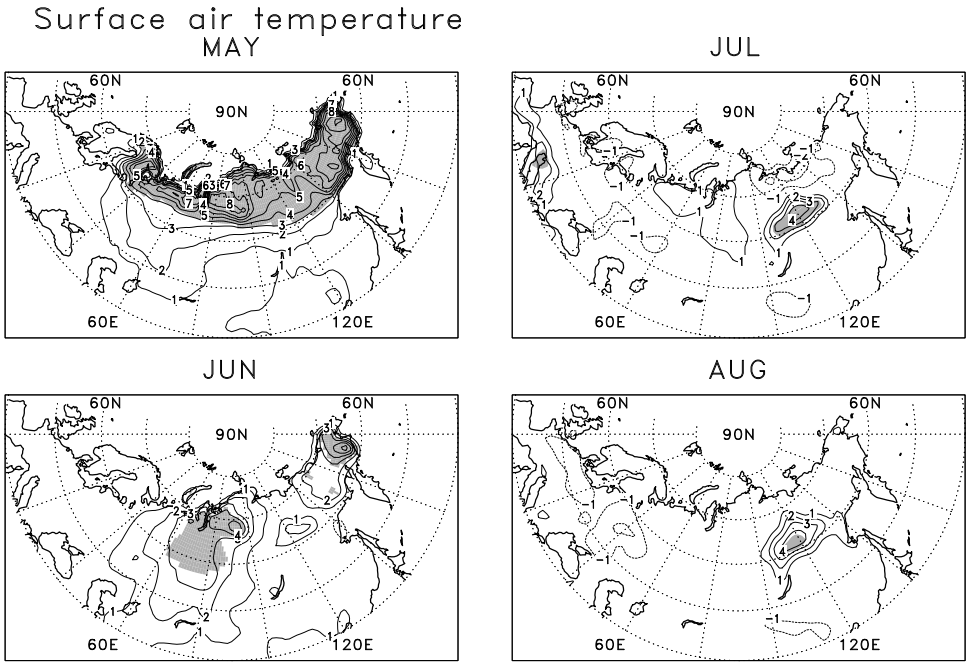

Figure 5. Surface air temperature anomalies (°C) between the light and heavy snow runs (light – heavy) from May to August. Regions showing a significance level above 90%, which is calculated by a t -test, are shaded.

heavy snow run (Figure 6a) in June corresponds to the simulated snow area (Figure 4b) over northern Siberia. In early summer, the Arctic Ocean iscovered with sea ice, and T_S is maintained at around 0°C (Figure 2). The albedo anomalies (Figure 6b) between the light and heavy snow runs show negative values in western Siberia, where T_S anomalies are positive in June, associated with the anomalous snow mass. The net solar radiation over northern Siberia shows a clear increase due to negative albedo anomalies during the snowmelt season (details are provided in the following subsection), which correspond to a springtime snow cover anomaly. The anomalous albedo of the snow cover allows surface heating, as anomalies in the snow mass remain present over northern Siberia in May and especially over western Siberia in June. Changes in atmospheric circulation also contribute to surface heating across broad regions (see section 4.1).

[14] In eastern Siberia (the Lena Basin), strong T_S anomalies remain in late summer (Figure 5). Snow disappearance occurs earlier in the Lena Basin at around 60°N than in western Siberia (Figures 1 and 4b), and albedo signals are not found after May. Thus, T_S anomalies in the Lena Basin cannot be explained in terms of the snow albedo effect.

[15] The anomalous snow mass also generates soil moisture anomalies (Figure 7). A large negative anomaly is maintained in eastern Siberia throughout summer, in agreement with the large positive T_S anomaly found at around 120°E. Ground wetness anomalies appear to play an important role in the development of T_S anomalies in eastern Siberia, whereas T_S anomalies in western Siberia are driven mainly by snow albedo anomalies. The ground wetness anomalies are produced by snow mass anomalies; however, the snow mass anomalies

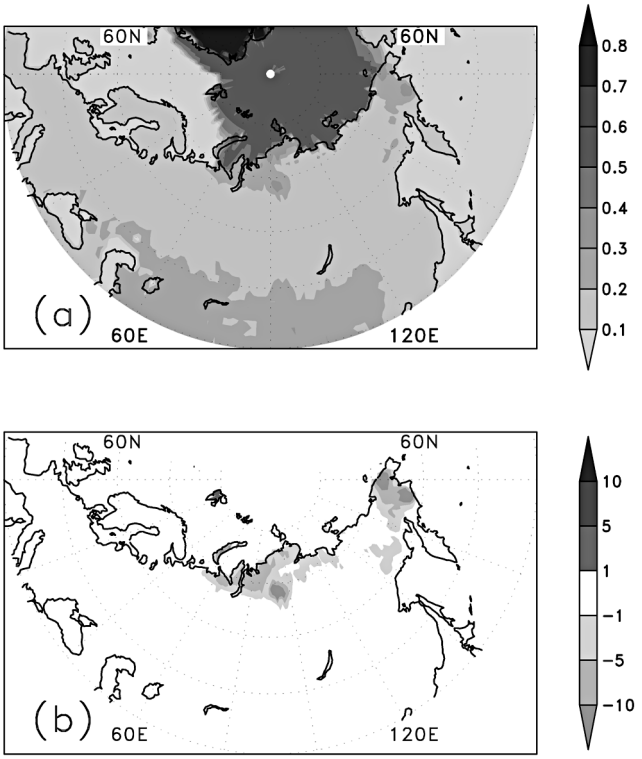

Figure 6. Distribution of albedo in the (a) heavy snow run in June and (b) the anomalies (%) between the light and heavy snow runs in June.

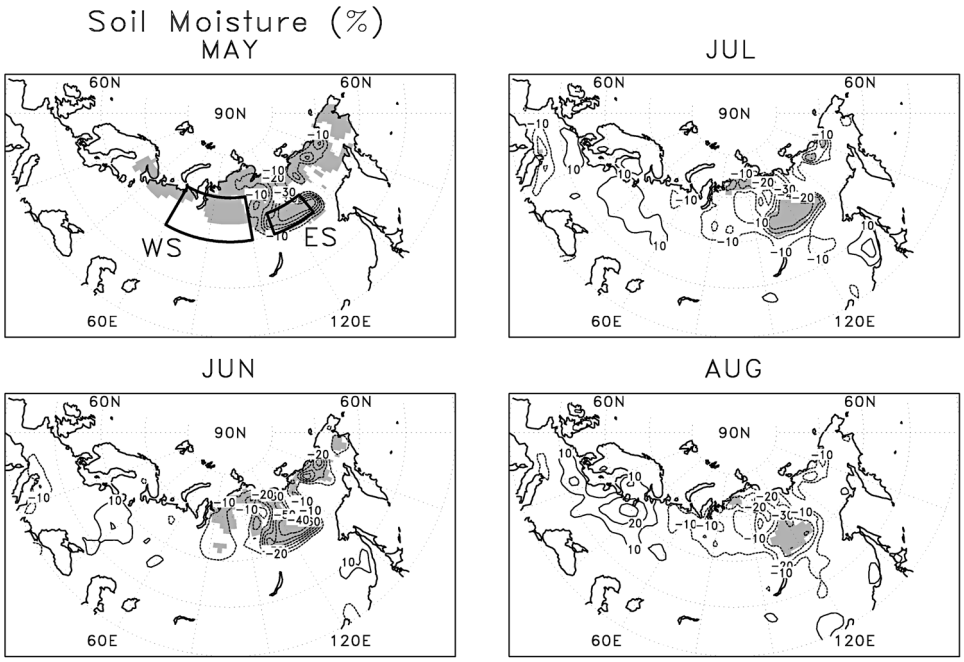

Figure 7. Same as Figure 5, but for soil moisture anomalies (%). Regions surrounded by thick solid lines are defined as western Siberia (WS; 60°N–70°N, 60°E–100°E) and eastern Siberia (ES; 60°N–65°N, 110°E–130°E).

are much greater in western Siberia than in the Lena Basin (Figures 3 and 4). This finding is discussed in detail below.

3.2. Heat and Water Budgets in Western and Eastern Siberia

[16] The various components of the surface heat and water budgets are examined to explain the T_S anomalies discussed above. Figure 8 shows monthly variations in surface heat fluxes and those of the anomalies in the light and heavy snow runs averaged over western Siberia (Figure 7; WS: 60°N–70°N, 60°E–100°E) and eastern Siberia (Figure 7; ES: 60°N–65°N, 110°E–130°E). The heat budget equation can be written as follows:

$$R_S + R_L + F_S + F_W + G = 0, \tag{4}$$

where R_S is solar radiation, R_L is long-wave radiation, F_S is sensible heat flux, F_W is latent heat flux, and G is ground heat conduction (including snowmelt energy). For the heat flux anomalies between the light and heavy snow runs, equation (4) is also written for the anomalies as

$$\Delta R_S + \Delta R_L + \Delta F_S + \Delta F_W + \Delta G = 0. \tag{5}$$

[17] In May, the R_S increases as a result of the reduced snow cover in the light snow run. At the same time, the reduced snow mass results in positive ΔG (mainly reduced snowmelt energy). The increased solar radiation and reduced snowmelt energy, which account for the significant increase in surface heating, balance the increased fluxes of R_L, F_W, and F_S in both regions.

[18] In western Siberia, the heat flux anomalies (light – heavy snow runs) continue to June, weaken in July, and disappear in August (Figure 8c), consistent with a gradual decrease of T_S anomaly there (Figure 5). However, in eastern Siberia, the F_W anomaly (ΔF_W: light – heavy snow runs) changes its sign in June and afterward, which means the evaporation in the light snow run decreases compared with that in the heavy snow run. To balance the decreased F_W, the F_S in the light snow run increases compared with that in the heavy snow run; thus the magnitude of ΔF_S increases after June (Figure 8f). This is led by dry surface conditions in the light snow run (Figure 7), as shown in the following, and contributes to heating of the atmosphere near the surface in summer.

[19] Moreover, the solar flux anomaly (ΔR_S) becomes large in July and August (Figure 8f), which suggests cloudiness anomalies in eastern Siberia in July and August. Figure 9 shows the cloudiness anomalies. In May, cloudiness along the Siberian coast decreases in the light snow run, contributing to the R_S increase in the light snow run. As expected, the cloudiness anomalies in eastern Siberia become negative in July and August, which contributes to the mid-summer positive ΔR_S in eastern Siberia (Figure 8f). The seasonal variations of the heat flux anomalies are greatly different in western and eastern Siberia (Figures 8c and 8f), resulting in contrasting responses of the T_S anomalies (Figure 5).

[20] Now we examine the surface water budget. Figure 10 shows the monthly time variations in the surface water budget. As described in section 2.1, the change in the sum of soil moisture and snow mass is equal to the sum of precipitation, evaporation, and runoff ($P - E - R$). In western Siberia, most of the runoff (Figure 10b) is driven by snowmelt (Figure 10d), as the soil is nearly saturated in both runs during the melting period (Figure 10c). The initial soil moisture content is 196.1 mm in western Siberia on May 1.

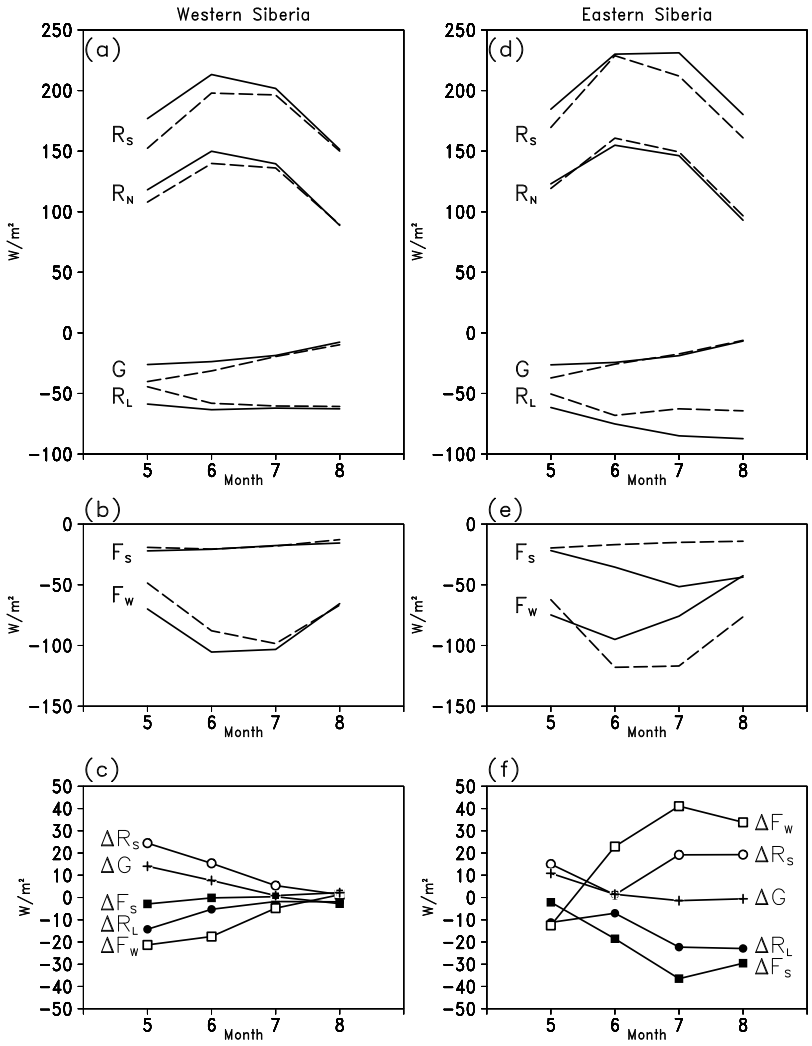

Figure 8. Monthly time variation of surface heat fluxes (W m^{-2}). (a) Net downward solar radiation flux (R_S), net downward long-wave radiation flux (R_L), net radiation flux (R_N), and ground heat conduction (G) in the light (solid line) and heavy (dashed line) snow runs. (b) Downward sensible heat flux (F_S) and downward latent heat flux (F_W). (c) Those of the anomalies between the light and heavy snow runs (light – heavy) averaged over western Siberia. (d–f): same as Figures 8a, 8b, and 8c but averaged over eastern Siberia.

This value decreases slowly, but in both runs it remains above 50% (100 mm) in August. This occurs because of the small difference in the rate of precipitation and evaporation (Figure 10a) throughout summer in both runs, although the evaporation is higher than the precipitation during the melting period in the light snow run (shaded column and solid line in Figure 10a).

[21] Since the initial soil moisture content in eastern Siberia is only 55.3 mm on May 1, snowmelt water can infiltrate into the soil. The initial snow mass is 22.2 mm in the light snow run and is 200.0 mm in the heavy snow run (Figures 3b and 3c). Therefore, the difference in initial snow mass between the light and heavy snow runs leads to large differences in soil moisture in May, and the difference in soil moisture remains large even after the snowmelt period (Figure 10g). Evaporation is generally larger than precipitation in eastern Siberia (Figure 10e, particularly in June and July), thus soil moisture rapidly decreases during summer. This also promotes the soil moisture decrease after snowmelt in both runs. Particularly in the light snow run, the soil moisture becomes quite small in July and August. Since evaporation efficiency decreases with decreasing soil wetness, the evaporation in the light snow run becomes much smaller than in the heavy snow run despite the increased ground temperature in the light snow run. Since the local evaporation contributes to the local precipitation very much in eastern Siberia (i.e., recycled water) [e.g., *Koster et al.*, 1986; *Numaguti*, 1999; *Serreze et al.*, 2003; *Kurita et al.*, 2004], the precipitation anomalies are similar to the evaporation anomalies, thereby maintaining the soil moisture anomalies between light and heavy snow runs.

[22] This snow-hydrological effect [e.g., *Barnett et al.*, 1989; *Yasunari et al.*, 1991] may be enhanced and maintained near the surface due to reduced cloudiness and precipitation in eastern Siberia; as a result of this effect, increased net solar radiation and decreased soil moisture

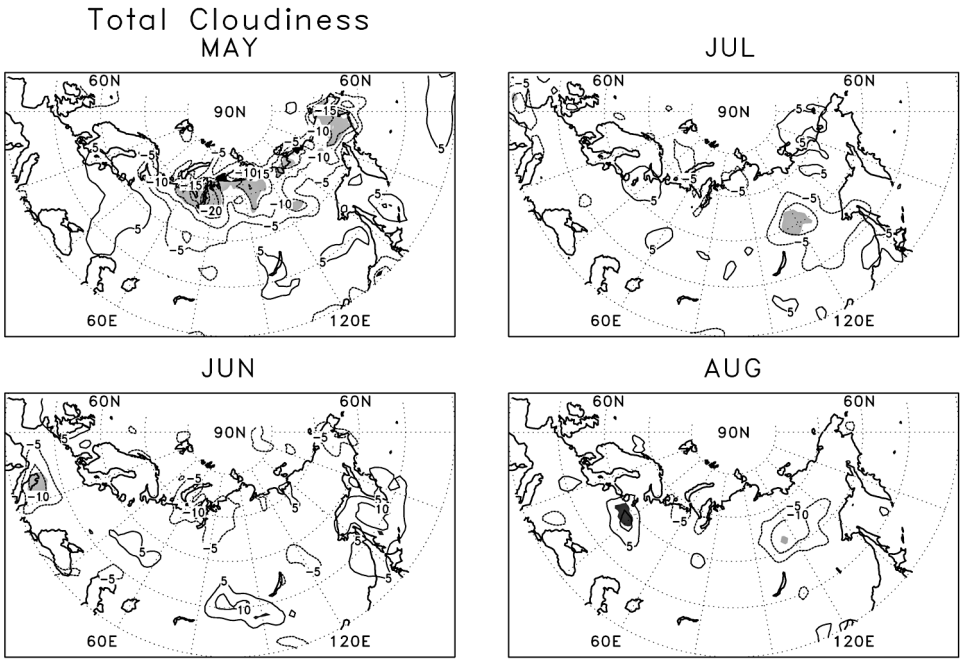

Figure 9. Same as Figure 5 but for total cloudiness anomalies (%). Dark shade: Positive values; light shade: Negative values.

content are maintained. Thus, the combination of the snow-hydrological effect (water mass) and coupling between evaporation and precipitation (water fluxes) appears to dominate the summer climate in eastern Siberia. A positive T_S anomaly is generated as a result of the difference between surface heating due to dry ground conditions (light snow run) and surface cooling due to wet ground conditions (heavy snow run) throughout summer. This snow-hydrological effect is more pronounced in July and August than in June. The above findings suggest that the effect of snow mass varies with the season, geographical location [e.g., *Barnett et al.*, 1989; *Yasunari et al.*, 1991; *Koster et al.*, 2004], and initial soil moisture content, among other factors.

4. Changes in Atmospheric Circulation and the Hydrological Cycle

4.1. Changes in Atmospheric Circulation

[23] The simulated T_S in northern Siberia reaches a maximum in July, when the land-sea T_S contrast across the Arctic coast is strongest (not shown). Figure 11 shows the monthly meridional 850-hPa temperature gradient ($\partial T/\partial y$) anomalies between the light and heavy snow runs. The anomalies increase along the Arctic coast in May (dashed contours), over western Siberia in June, and over eastern and northeastern Siberia in July and August. These strong negative anomalies over land agree with the enhanced T_S anomalies (Figure 5); the negative anomalies in eastern Siberia extend eastward in July and August.

[24] The strong temperature gradient affects the upper tropospheric westerly via the thermal wind relationship. Figure 12 shows the monthly 300-hPa zonal wind in the light snow run and the wind anomalies (light – heavy snow runs). Although the subtropical jet becomes weaker as the season progresses, the subpolar jet forms along the Arctic coast (from the North Atlantic to western Siberia) in May, extends southeastward in June, and strengthens over eastern and northeastern Siberia in July, forming a double-jet structure with the subtropical jet. The westerly anomalies corresponding to the subpolar jet are also enhanced over eastern and northeastern Siberia in August. These increased westerlies correspond to the strong temperature gradient. Thus, these results suggest that the snow-hydrological effect in eastern Siberia acts to maintain the westerly anomalies over eastern and northeastern Siberia in July and August.

[25] Figure 13 shows latitude-pressure sections of the zonal wind in both runs and of the anomalies in July. The subpolar jet and subtropical jet are clearly seen in the upper troposphere in the light snow run (solid contours). In addition, westerly anomalies strengthen from the lower to the upper troposphere over the Arctic coast. These results are consistent with those obtained by *Ogi et al.* [2004], who found that an enhanced thermal contrast along the Arctic coast results in increased zonal wind and eddy activity, which in turn maintains the summertime Northern Hemisphere annular mode (NAM).

[26] Figure 14 shows monthly 300-hPa geopotential height anomalies and associated wave-activity fluxes as defined by *Takaya and Nakamura* [2001]. Positive anomalies are found over the snow zone in May. In June, strong anomalies are seen over western Siberia, and wave activity emanates eastward in the form of a stationary Rossby wave packet from around 60°E across western Siberia. Development of the Rossby wave also occurs in July, with northward translation of the wave pattern by 10°. The Rossby wave may contribute to the formation of an upper-level ridge above the surface Okhotsk high, although it is located slightly to the east. In August, there is no significant change in wave propagation. The geopotential height anomalies

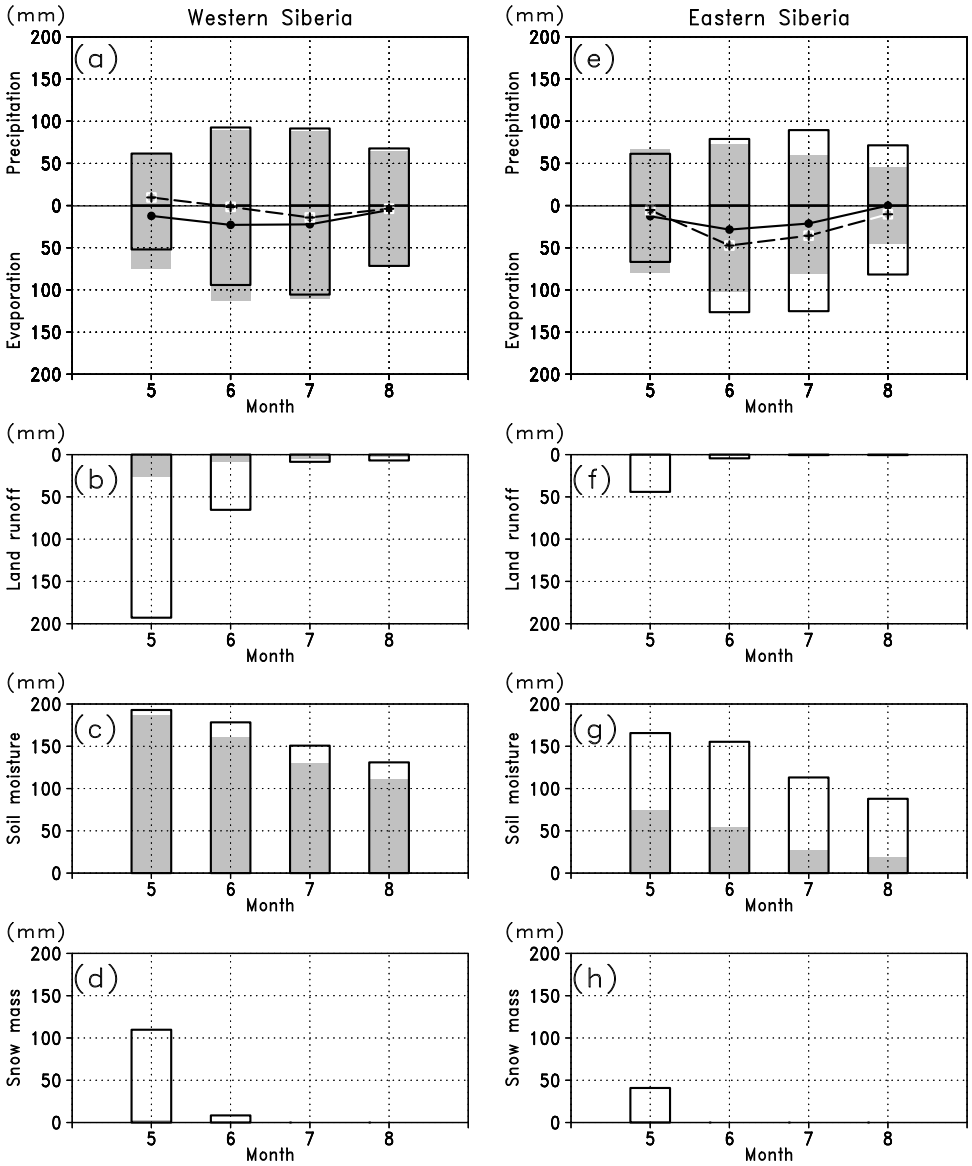

Figure 10. Monthly time variation of surface water budget (mm). (a) Precipitation (P), evaporation (E) in the light (shaded column) and heavy (solid column) snow runs, and P – E (light snow run: solid line; heavy snow run: dashed line). (b) Land runoff. (c) Soil moisture. (d) Snow mass averaged over western Siberia. (e–h): Same as Figures 10a, 10b, 10c, and 10d but averaged over eastern Siberia.

show a near-equivalent barotropic structure from the lower to upper troposphere throughout summer (not shown).

[27] The above results suggest that enhanced westerlies form a subpolar jet and that the wave activity that accompanies the subpolar jet as a waveguide is enhanced by the increase in surface heating that occurs as a consequence of anomalous snow cover in northern Eurasia. Another Rossby wave appears to propagate northeastward in June over eastern Siberia, where marked T_S anomalies act as a strong heating source. The wave disappears in July but is faintly visible in August. Overall, the eastward wave activity appears to dominate the upper atmosphere over northern Eurasia.

4.2. Changes in the Hydrological Cycle

[28] Changes in atmospheric circulation result in anomalous hydrological cycles. Figure 15 shows the moisture flux and precipitation anomalies. The moisture fluxes represent the stationary moisture fluxes calculated from monthly mean atmospheric fields, and vertical integrations from the surface to 300-hPa level. The transient fluxes are unavailable, as we did not output daily values. Nevertheless, the stationary component is dominant over northern Eurasia in summer [e.g., *Tachibana et al.*, 2008]. Cyclonic circulation accompanied by a negative height anomaly generates positive precipitation anomalies around 40°E over western Russia in June and July. The increased northward moisture transport contributes to the precipitation anomalies in western Russia. Increased precipitation, accompanied by cyclonic circulating moisture flux anomalies, appears over western Russia in August. As discussed previously, reduced precipitation occurs over eastern Siberia in June and continues until

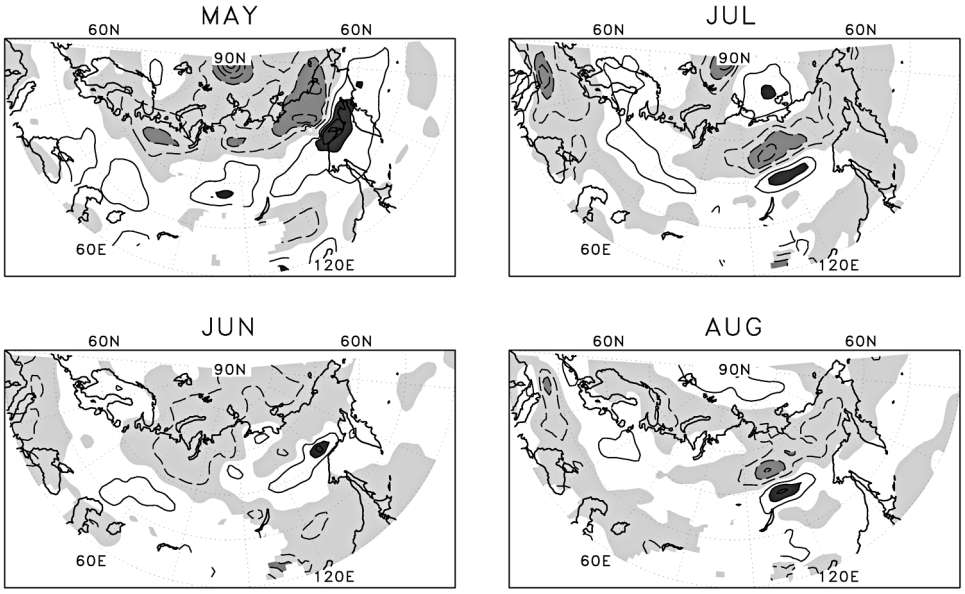

Figure 11. Monthly meridional 850-hPa temperature gradient anomalies (solid contours: positive values; dashed contours: negative values) between the light and heavy snow runs from May to August. The contour interval is 2×10^{-4} K km^{-1} with the zero contour omitted. Light shading indicates negative values, medium and heavy shading indicates absolute values exceeding 4×10^{-4} K km^{-1}.

August. Anortherly moisture flux anomaly and anticyclonic circulation to the east are apparent in July and August.

[29] Tables 1 and 2 show the atmospheric water budgets over western Russia (55°N–65°N, 30°E–60°E) and eastern Siberia (60°N–65°N, 110°E–130°E). Both regions lie mainly within moisture-divergent fields, except over western Russia in May and August in the light snow run. Both positive evaporation and moisture convergence anomalies contribute to increased precipitation over western Russia. The evaporation anomalies are comparable to the moisture convergence anomalies in August. In contrast, precipitation in eastern Siberia is dominated by evaporation variability, as recycled

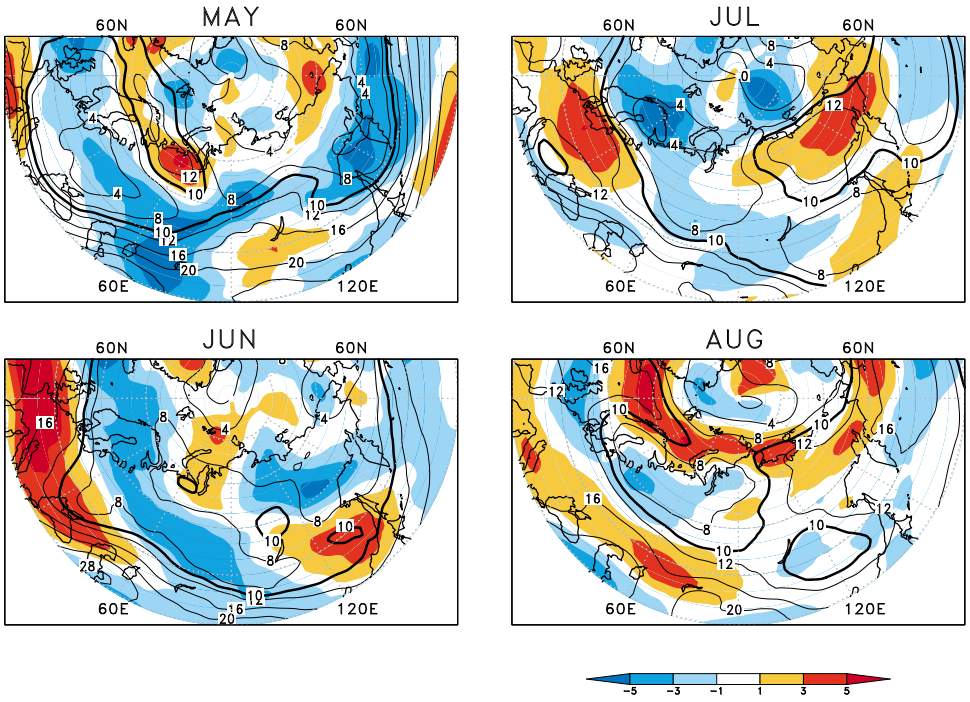

Figure 12. Monthly 300-hPa zonal wind (m s^{-1}) in the light snow run (solid contours) and that of the anomalies (shaded) between the light and heavy snow runs from May to August. The bold solid contours indicate 10 m s^{-1}.

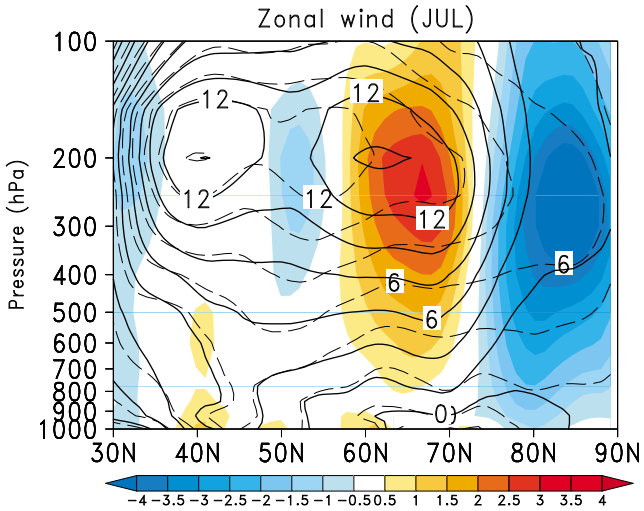

Figure 13. Latitude pressure sections of zonal wind (m s^{-1}) in the light (solid contours) and heavy (dashed contours) snow runs and their anomalies (shaded) in July, zonally averaged from 90°E to 180°E.

water is the moisture source for convective precipitation. In both regions, the evaporative effect in late summer is stronger than that in early summer.

[30] As mentioned above, an east–west dipole structure of circulation and precipitation anomalies is found over northern Eurasia (Figures 14 and 15). This dipole signature is also found in T_S (Figure 5), soil moisture (Figure 7), cloudiness (Figure 9), and cumulus precipitation (not shown) anomalies in July and August. *Fukutomi et al.* [2003] reported that the precipitation variance has two centers of action in the summer: one over eastern Siberia and the other over western Russia. They also found that a regression analysis on the basis of the precipitation index for the Lena and Ob rivers shows an east–west dipole structure similar to that shown in Figure 15. Therefore, there is a possibility that the observed dipole structure is caused by snow anomalies via land-atmosphere interactions, which act to change the summertime precipitation patterns over the two basins. Further research is required to better understand the formation of the dipole structure.

5. Discussion

[31] The present findings indicate that variations in springtime Eurasian snow cover result in variations in summertime northern atmospheric circulation and the hydrological cycle via land-atmosphere interactions. Thus, the springtime Eurasian snow mass is expected to be an important factor in predicting the northern summer climate. *Ogi et al.* [2003] pointed out that springtime Eurasian snow cover is affected by the previous winter NAO. Likewise, *Schaefer et al.* [2004] noted that the wintertime AO influences the timing of snow disappearance in northern Europe and eastern Siberia. Therefore, the wintertime and springtime atmospheric conditions that lead to the formation of anomalous snow mass have a strong influence on the summertime high-latitude climate.

[32] A Rossby wave appears to propagate northeastward over eastern Siberia, where strong T_S anomalies act as a strong heating source. *Wang and Yasunari* [1994] found that a Rossby wave emanates from eastern Siberia and propagates into the subtropical region of the Pacific in early

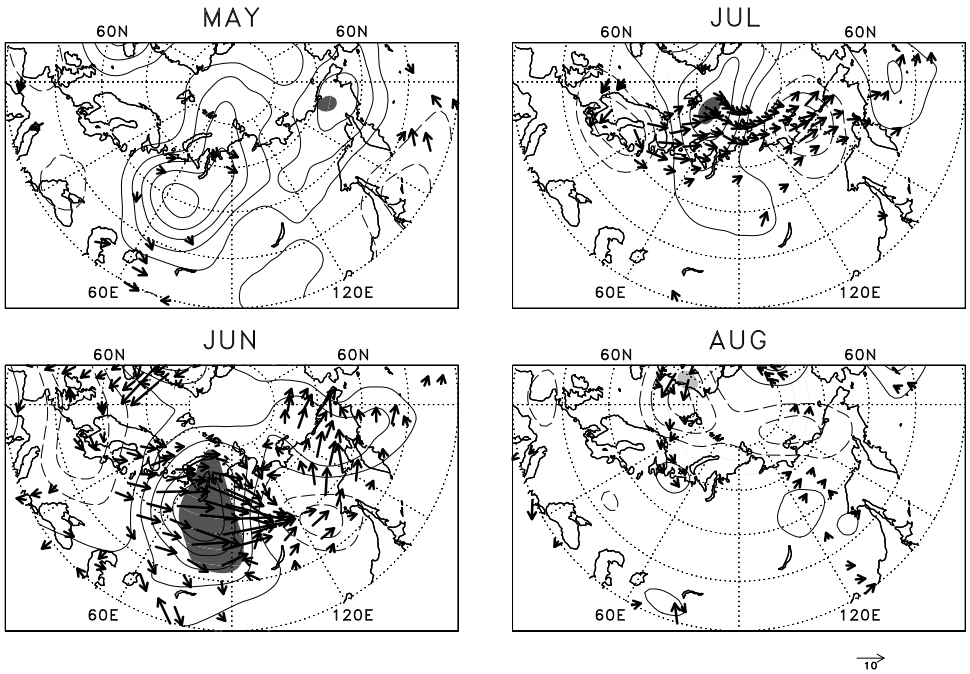

Figure 14. Monthly 300-hPa geopotential height anomalies (contours at intervals of 20 m) and associated wave activity fluxes (arrows: m^{-2} s^{-2}), as defined by *Takaya and Nakamura* [2001]. Solid contours indicate positive values, and dashed contours indicate negative values. Regions showing a significance level above 90% are shaded.

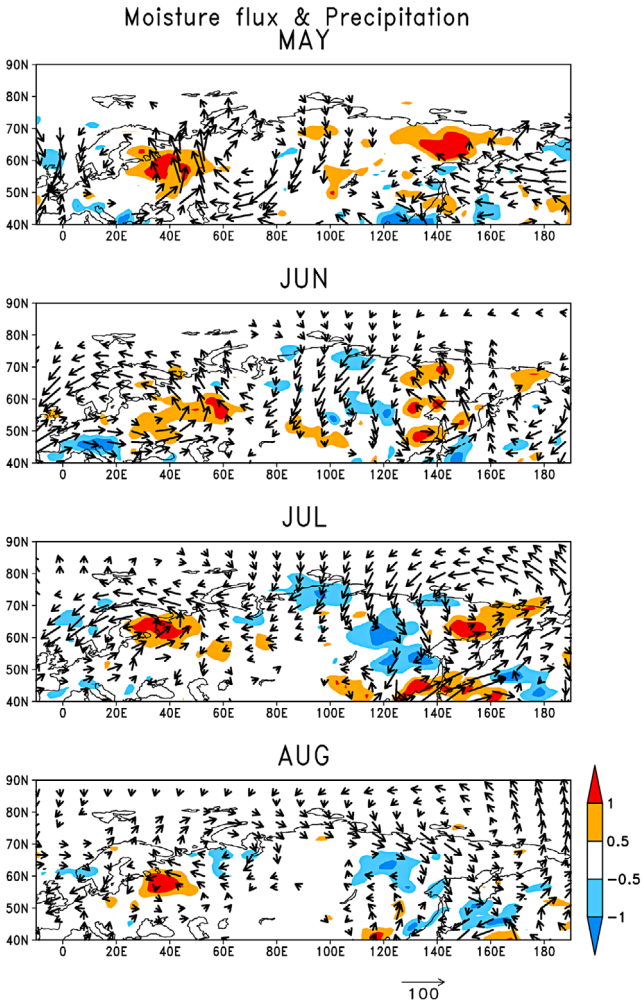

Figure 15. Stationary moisture fluxes (arrows: kg m^{-1} s^{-1}) and precipitation anomalies (shaded: mm day^{-1}) between the light and heavy snow runs from May to August.

summer. They suggested that eastern Siberia is one of the important forcing sources of quasi-stationary waves. The snow-hydrological effect in eastern Siberia maintains westerly anomalies until August and appears to act as a forcing source of stationary waves, which may affect the formation of an upper-level ridge above the surface Okhotsk high.

[33] The initial soil moisture is almost saturated in western Siberia on May 1, but not in eastern Siberia. In eastern Siberia in particular, the occurrence of rapid snowmelt means that soil moisture shows a rapid increase in May and a decrease in summer. The dry ground conditions in spring, which is affected by anomalous snow mass, are the most important factors in terms of the snow-hydrological effect in eastern Siberia. In contrast, the wet ground conditions in western Siberia mean that the response to the anomalous snow mass is not much more sensitive than the response in eastern Siberia. Thus, the albedo effect, which is affected by the extent of anomalous snow cover, is significant in western Siberia, whereas the snow-hydrological effect is not.

[34] The soil moisture and surface evaporation anomalies are sustained by increased convective precipitation, thereby

Table 1. Precipitation (P), Evaporation (E), Stationary Moisture Flux Convergence ($-\nabla Q$), and Anomalies Over Western Russia (55°N–65°N, 30°E–60°E)[a]

	Western Russia								
	Anomaly			Light Snow Run			Heavy Snow Run		
	P	E	$-\nabla Q$	P	E	$-\nabla Q$	P	E	$-\nabla Q$
May	0.73	**0.37**	**1.28**	2.72	3.26	0.15	1.99	2.89	−1.13
Jun	0.47	0.12	0.36	3.37	4.14	−0.44	2.90	4.02	−0.80
Jul	0.63	0.23	0.29	3.23	3.93	−0.50	2.60	3.70	−0.79
Aug	**0.44**	0.30	0.31	2.72	2.66	0.19	2.28	2.36	−0.12

[a]The unit of measurement is mm day^{-1}. The bold type indicates a significance level above 90%.

indicating a coupling between evaporation and convection. However, the snow-hydrological effect in our model appears to be highly effective in terms of heating in the lower troposphere, as also reported by *Yasunari et al.* [1991]. This characteristic nature of the model response to the anomalous snow mass and wet ground appears to be closely associated with the cumulus parameterization of *Arakawa and Schubert* [1974], in which cumulus convection is highly sensitive to evaporation, or more directly, the amount of moisture in the planetary boundary layer.

[35] *Takata and Kimoto* [2000] considered the fact that the impermeability of frozen soil to spring meltwater leads to increased runoff; consequently, summer soil wetness is significantly reduced, resulting in turn in an increase in summertime surface temperatures over the boreal continents. Because the present study is concerned mainly with seasonal land-atmosphere interactions, we focused on soil moisture in the shallow soil layer. Thus, we used a one-layer model for soil moisture. To consider the role of frozen soil, it is necessary to use a multilayer model. Further research is required to understand the influence of frozen soil on land-atmosphere interactions and seasonal variation in soil moisture in northern Eurasia.

6. Conclusions

[36] We used an AGCM to assess the effect of springtime anomalous snowcover in northern Eurasia on the summertime land-atmosphere climate system. Light and heavy snow runs were performed to study changes in the initial snow mass in northern Eurasia. Significant differences in the model responses of two runs are evident in terms of not only land surface parameters but also summertime high-latitude atmospheric circulation. The main results of this study are summarized as follows.

[37] 1. In western Siberia (60°N–70°N, 60°E–100°E), the albedo of snow cover makes a large contribution to surface

Table 2. Same as Table 1 but Averaged Over Eastern Siberia (60°N–65°N, 110°E–130°E)

	Eastern Siberia								
	Anomaly			Light Snow Run			Heavy Snow Run		
	P	E	$-\nabla Q$	P	E	$-\nabla Q$	P	E	$-\nabla Q$
May	0.20	**0.44**	0.02	2.15	2.57	−0.37	1.95	2.13	−0.39
Jun	−0.17	**−0.82**	0.22	2.34	3.24	−0.87	2.51	4.06	−1.09
Jul	**−0.95**	**−1.47**	0.05	1.90	2.56	−1.00	2.85	4.03	−1.05
Aug	**−0.85**	**−1.18**	0.02	1.44	1.43	−0.86	2.29	2.61	−0.88

heating by late June, as snow mass anomalies are still present. The net radiation shows an increase as a result of the difference between the extent of snow cover in the light and heavy snow runs; this radiation and reduced snowmelt energy, which account for the significant increase in surface heating, balance the increased latent and sensible heat fluxes. After snowmelt, the climate signals become weaker.

[38] 2. In eastern Siberia (60°N–65°N, 110°E–130°E), the snow-hydrological effect is significant throughout summer. In the heavy snow run, the increase in soil moisture content results in surface cooling via increased evaporation. T_S anomalies are generated as a result of the difference between surface heating due to dry ground conditions (light snow run) and surface cooling due to wet ground conditions (heavy snow run). This difference in the model response between eastern and western Siberia arises mainly from differences in their initial soil moisture contents (the initial content is lower in eastern Siberia).

[39] 3. Following strong surface heating over northern Eurasia, the subpolar jet is strengthened and maintained along the Arctic coast in the upper troposphere, and wave activity emanates eastward in the form of a stationary Rossby wave packet during early summer. An atmospheric circulation anomaly, together with the difference in the initial soil moisture content, generates an east–west dipole structure of precipitation anomalies over northern Eurasia.

[40] **Acknowledgments.** We thank M. Kimoto and S. Minobe, M. Watanabe, T. Enomoto, T. Nishimura, and N. Kurita for their helpful comments. We also thank three anonymous reviewers for providing useful comments for the improvement of this paper. Major computational resources were provided by FRCGC. Figures were drawn using GrADS software.

References

Arai, M., and M. Kimoto (2005), Relationship between Springtime surface temperature and early summer blocking activity over Siberia, *J. Meteorol. Soc. Jpn.*, *83*, 261–267.

Arakawa, A., and W. H. Schubert (1974), Interaction of a cumulus cloud ensemble with the large-scale environment Part I., *J. Atmos. Sci.*, *31*, 674–701.

Barnett, T. P., L. Dümenil, U. Schlese, and E. Roeckner (1989), The effect of Eurasian snow cover on regional and global climate variatoins, *J. Atmos. Sci.*, *46*, 661–685.

Bojariu, R., and L. Gimeno (2003), The role of snow cover fluctuations in multiannual NAO persistence, *Geophys. Res. Lett.*, *30*(4), 1156, doi:10.1029/2002GL015651.

Douville, H., and J.-F. Royer (1996), Sensitivity of the Asian summer monsoon to an anomalous Eurasian snow cover within the Météo-France GCM, *Clim. Dyn.*, *12*, 449–466.

Fukutomi, Y., H. Igarashi, K. Masuda, and T. Yasunari (2003), Interannual variability of summer water balance components in three major river basins of northern Eurasia, *J. Hydrometeorol.*, *4*, 283–296.

Groisman, P. Y., T. R. Karl, and R. W. Knight (1994), Observed impact of snow cover on the heat balance and the rise of continental spring temperatures, *Science*, *263*, 198–200.

Iijima, Y., K. Masuda, and T. Ohata (2007), Snow disappearance in eastern Siberia and its relationship to atmospheric influences, *Int. J. Climatol.*, *27*, 169–177, doi:10.1002/joc.1382.

Kalnay, E., M. Kanamitsu, and co-authors (1996), The NCEP/NCAR 40-year reanalysis project, *Bull. Amer. Meteorol. Soc.*, *77*, 301–326.

Kodera, K., and M. Chiba (1989), West Siberian spring snow cover and East Asian June 500 hPa Height, *Pap. Meteor. Geophys.*, *40*, 51–54.

Koster, R. D., J. Jouzel, R. Suozzo, G. Russell, W. Broecker, D. Rind, and P. Eagleson (1986), Global sources of local precipitation as determined by the NASA/GISS GCM, *Geophys. Res. Lett.*, *13*, 121–124, doi:10.1029/GL013i002p00121.

Koster, R. D., et al. (2004), Regions of strong coupling between soil moisture and precipitation, *Science*, *305*, 1138–1140.

Kurita, N., N. Yoshida, G. Inoue, and E. A. Chayanova (2004), Modern isotope climatology of Russia: A first assessment, *J. Geophys. Res.*, *109*, D03102, doi:10.1029/2003JD003404.

Nakamura, H., and T. Fukamachi (2004), Evolution and dynamics of summertime blocking over the Far East and the associated surface Okhotsk high, *Q. J. R. Meteorol. Soc.*, *130*, 1213–1233.

Numaguti, A. (1999), Origin and recycling processes of precipitating water over the Eurasian continent: Experiments using an atmospheric general circulation model (1999), *J. Geophys. Res.*, *104*, 1957–1972, doi:10.1029/1998JD200026.

Ogi, M., Y. Tachibana, and K. Yamazaki (2003), Impact of the wintertime North Atlantic Oscillation (NAO) on the summertime atmospheric circulation, *Geophys. Res. Lett.*, *30*(13), 1704, doi:10.1029/2003GL017280.

Ogi, M., K. Yamazaki, and Y. Tachibana (2004), The summertime annular mode in the Northern Hemisphere and its linkage to the winter mode, *J. Geophys. Res.*, *109*, D20114, doi:10.1029/2004JD004514.

Schaefer, K., A. S. Denning, and O. Leonard (2004), The winter Arctic oscillation and the timing of snowmelt in Europe, *Geophys. Res. Lett.*, *31*, L22205, doi:10.1029/2004GL021035.

Serreze, M. C., A. H. Lynch, and M. P. Clark (2001), The Arctic frontal zone as seen in the NCEP-NCAR reanalysis, *J. Clim.*, *14*, 1550–1567.

Serreze, M. C., D. H. Bromwich, M. P. Clark, A. J. Ertringer, T. Zhang, and R. Lammer (2003), Large-scale hydro-climatology of the terrestrial Arctic drainage system, *J. Geophys. Res.*, *108*(D2), 8160, doi:10.1029/2001JD000919.

Shen, X., M. Kimoto, and A. Sumi (1998), Role of land surface processes associated with interannual variability of broad-scale Asian summer monsoon as simulated by the CCSR/NIES AGCM, *J. Meteorol. Soc. Jpn.*, *76*, 217–236.

Shinoda, M., H. Utsugi, and W. Morishima (2001), Spring snow-disappearance timing and its possible influence on temperature fields over central Eurasia, *J. Meteorol. Soc. Jpn.*, *79*, 37–59.

Tachibana, Y., T. Iwamoto, M. Ogi, and Y. Watanabe (2004), Abnormal meridional temperature gradient and its relation to the Okhotsk High, *J. Meteorol. Soc. Jpn.*, *82*, 1399–1415.

Tachibana, Y., K. Oshima, and M. Ogi (2008), Seasonal and interannual variations of Amur River discharge and their relationships to large-scale atmospheric patterns and moisture fluxes, *J. Geophys. Res.*, *113*, D16102, doi:10.1029/2007JD009555.

Takata, K., and M. Kimoto (2000), A numerical study on the impact of soil freezing on the continental-scale seasonal cycle, *J. Meteorol. Soc. Jpn.*, *78*, 199–221.

Takaya, K., and H. Nakamura (2001), A formulation of phase-independent wave-activity flux of stationary and migratory quasigeostrophic eddies on a zonally varying basic flow, *J. Atmos. Sci.*, *58*, 608–627.

Vernekar, A. D., J. Zhou, and J. Shukla (1995), The effect of Eurasian snow cover on the Indian monsoon, *J. Clim.*, *8*, 248–266.

Wang, Y., and T. Yasunari (1994), A diagnostic analysis of the wave train propagating from High-latitudes to Low-latitudes in early Summer, *J. Meteorol. Soc. Jpn.*, *72*, 269–279.

Yasunari, T., A. Kitoh, and T. Tokioka (1991), Local and remote responses to excessive snow mass over Eurasia appearing in the Northern Spring and Summer climate, *J. Meteorol. Soc. Jpn.*, *69*, 473–487.

S. Matsumura and K. Yamazaki, Faculty of Environmental Earth Science, Hokkaido University, Kita 10 Nishi 5, Sapporo 060-0810, Japan. (matsusnj@ees.hokudai.ac.jp)

T. Tokioka, Japan Agency for Marine-Earth Science and Technology, 3173-25 Showa-machi, Kanazawa-ku, Yokohama 236-0001, Japan.